NASA TECHNICAL MEMORANDUM

NASA TM X-1889

NASA TM X-1889

EFFECT OF ANGLE OF ATTACK AND INJECTION PRESSURE ON JET PENETRATION AND SPREADING FROM A DELTA WING IN SUPERSONIC FLOW

by Frederick P. Povinelli, Louis A. Povinelli, and Martin Hersch

Lewis Research Center
Cleveland, Ohio

NATIONAL AERONAUTICS AND SPACE ADMINISTRATION • WASHINGTON, D. C. • SEPTEMBER 1969

EFFECT OF ANGLE OF ATTACK AND INJECTION PRESSURE ON JET PENETRATION AND SPREADING FROM A DELTA WING IN SUPERSONIC FLOW

by Frederick P. Povinelli, Louis A. Povinelli, and Martin Hersch

Lewis Research Center

SUMMARY

Helium injection into the vortex flow generated over the lee side of a half-delta surface was studied in a Mach 2 airstream to determine the effect of angle of attack and injection pressure on jet penetration and spreading. This method of injection into the vortices formed over swept surfaces at angle of attack may have practical use in a supersonic combustion ramjet where fuel distribution appears to be a problem.

Angles of attack from 6^{o} to 18^{o} were studied with injection pressures of 15 and 60 psia (103.4 and 413.7 kN/m^2). Concentration contours were obtained at two positions downstream of the injection orifice. Oil streaks of the flow on the model surface were photographed and used to determine the position of the vortex with change in angle of attack.

Penetration and spreading of the injectant were enhanced as the angle of attack was increased. Increasing injection pressure increased the penetration but had little effect on spreading for the configuration tested. Maximum penetration occurred at the highest angle of attack and injection pressure tested. An increase in angle of attack increased penetration more than did an increase in injection pressure in the vortex region. However, in line with the injection orifice, injection pressure was more effective in increasing penetration.

INTRODUCTION

The injection, mixing, and efficient combustion of a fuel in a supersonic airstream remains a crucial problem which may impede the successful development of supersonic combustion ramjets. In the last several years considerable effort has been directed toward understanding the behavior of a nonreacting gas injected into a supersonic air-

stream. Several types of injection schemes which have been tried are sonic and supersonic injection through a circular hole perpendicular to the free stream (ref. 1), tangential slot injection (ref. 2), and the injection at an angle to the flow and multiple hole injection (ref. 3). Regardless of the scheme used, the penetration of the injectant has been limited, thus restricting engines to small combustor heights or long mixing lengths to achieve efficient fuel coverage of the flow area. Additional combustor length to accomplish the required fuel distribution and mixing can be achieved only at the expense of increased cooling requirements. Thus, injection from struts protruding into the free stream of a larger cross-section combustor would be a probable solution to the fuel distribution problem. The efficient design of a combustor would then represent a compromise between strut cooling difficulties and drag and the excessive frictional drag and cooling requirements of high length to diameter ratio combustor passages.

A technique has been employed recently (ref. 4) of injecting gas into the vortex flow generated over the lee side of a delta wing. The delta wing was studied as a possible strut configuration. A significant increase in the penetration was obtained with the delta when compared with that obtained from an unswept flat plate at the same angle of attack. (Penetration for the delta was measured along a mean vortex line while penetration for the flat plate was measured directly downstream from the injection orifice.) Also a twofold increase in lateral spreading was obtained with the delta when compared with that obtained with the flat plate in reference 4. The improved distribution depended on the vortex flow formed by the circulation of airflow from the high-pressure windward side of the delta to the lower pressure lee side. Injection from the lee side resulted in the gas being carried into the vortex flow and distributed over a greater region than was obtained with injection in the absence of vortices.

This study was performed to determine the effects of angle of attack and injection pressure on the penetration and spreading of a gas injected from the lee side of a half-delta injector.

The half-delta injector used for this study had a nominal 60° sweep back angle and was varied in angle of attack from 6° to 18°. The model was mounted in a Mach 2 airstream having a stagnation pressure of 0.92 atmosphere (93.1 kN/m^2) and a stagnation temperature of 625° R (347 K). Helium was injected from the lee side of the delta at total pressures of 15 and 60 psia (103.4 and 413.7 kN/m^2) and ambient temperature.

SYMBOLS

d injection orifice diameter

P_o injection total pressure

x distance measured from injection orifice parallel to free stream

y distance measured from model surface perpendicular to free stream at any x and θ position

α angle of attack

β vortex separation angle

ϵ model apex angle

θ angular position measured on model surface

σ vortex attachment angle

APPARATUS AND PROCEDURE

Model

The half-delta model used for this study is shown in figure 1. The model had a sharp leading edge with a sweep back angle of 58.5°. A 0.198-centimeter-diameter injection orifice was located 3.99-centimeters from the apex on a 14° line from the leading

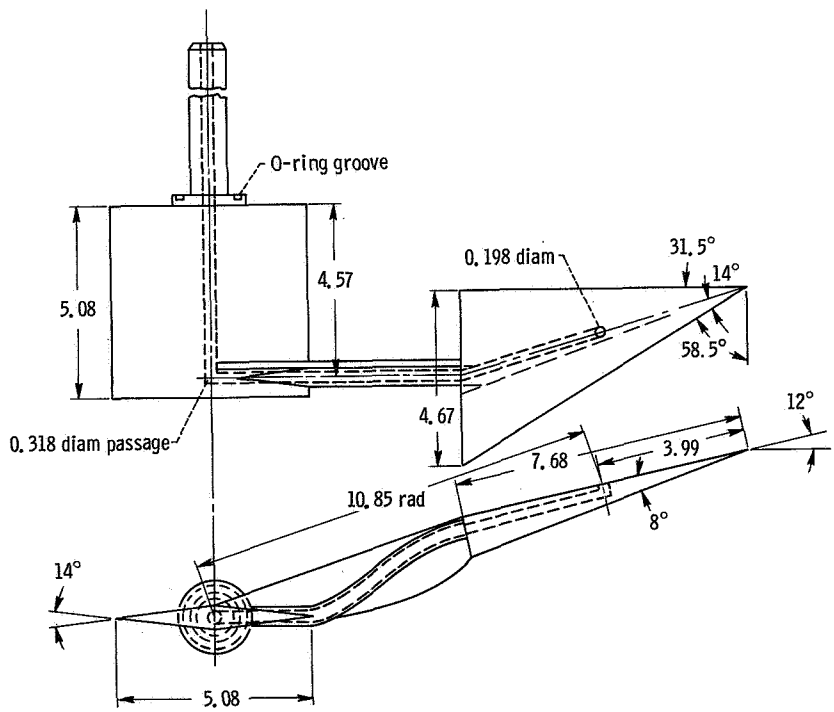

Figure 1. - Delta wing injector used for helium injection. (All linear dimensions are in centimeters.)

edge. The model was sting mounted from a diamond shaped strut. A 0.318-centimeter-diameter passage for injectant flow was provided through the strut, sting, and model to the injection orifice. A half-delta was used because a full delta would not allow the tunnel to start.

Wind Tunnel Configuration

The injector configuration was mounted through a side wall of a Mach 2 wind tunnel (fig. 2) and was positioned at angle of attack to the tunnel airflow by rotating the support

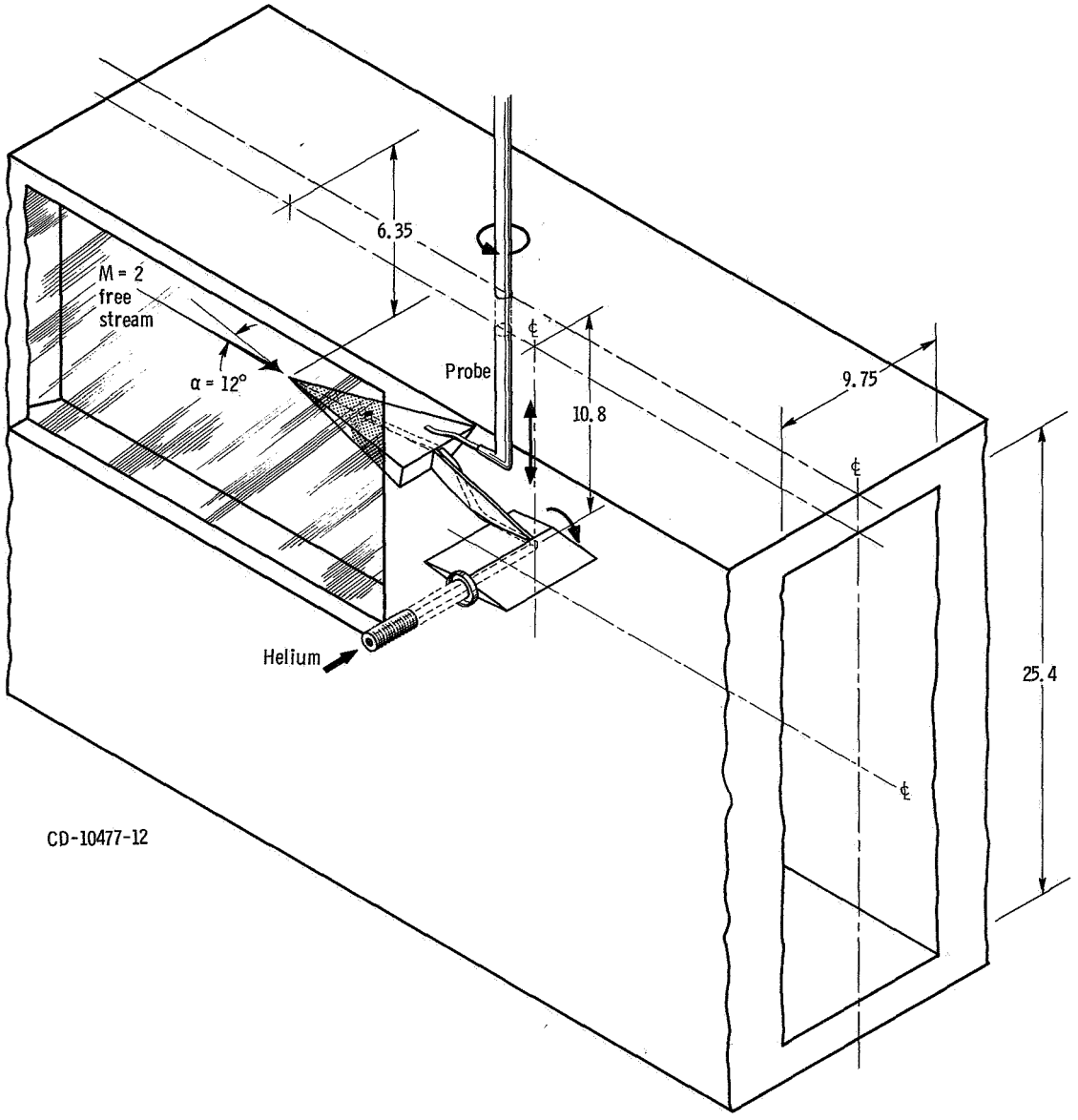

Figure 2. - Model location in tunnel at 12° angle of attack. (All linear dimensions are in centimeters.)

strut. The tunnel had a rectangular cross section of 25.4 by 9.75 centimeters. Air with a dewpoint of 244 K was heated to 347 K and allowed to flow through the tunnel at a stagnation pressure of 0.92 atmosphere (93.1 kN/m^2). The model was located outside of both the top and side wall tunnel boundary layers. Shock waves generated by the model surfaces reflected from the boundary layer downstream of the model trailing edge.

Vortex Visualization

In order to determine the behavior of the vortex flow over the lee side of the delta, a mixture of lampblack and linseed oil was painted on the top surface, and the resulting flow pattern photographed. Oil streaks were obtained at angles of attack of 6°, 9°, 12°, and 15°, with the injection orifice plugged, and at 12° and 18°, with injectant flow.

Helium Sampling

The method of helium injection and detection was essentially the same as that described in reference 4. A schematic of the injection system is shown in figure 3(a). Helium was injected normal to the model surface at total pressures P_o of 15 and 60 psia (103.4 and 413.7 kN/m^2) at ambient temperature. Two probes with identical tip configurations were used to sample the helium-air mixtures (fig. 3(b)); the difference in the probes was the distance from the tip to the rotation axis. The gas sample was fed into an on-line helium detection system (fig. 3(c)). The helium concentration output was displayed on an x-y plotter. Calibration with known mixtures of helium determined the output to be linear with helium concentration, and the reproducibility to be ±5 percent at full scale (i.e., 100 percent helium).

Measurement Locations

Helium concentration measurements were taken from the model surface upward until helium was no longer detected. Traverses were made at various angular positions, at two downstream locations, for five angles of attack. Two injection pressures were used.

In order to facilitate lateral positioning of the probe, lines were scribed on the delta top surface at angular positions θ in 5° increments (fig. 4). The arcs resulting from probe rotations are depicted in the top view schematic and are labeled x-station 1 and x-station 2. The x-coordinate was measured parallel to the tunnel free-stream flow direction, with the origin at the center of the injection orifice. The probe was moved in

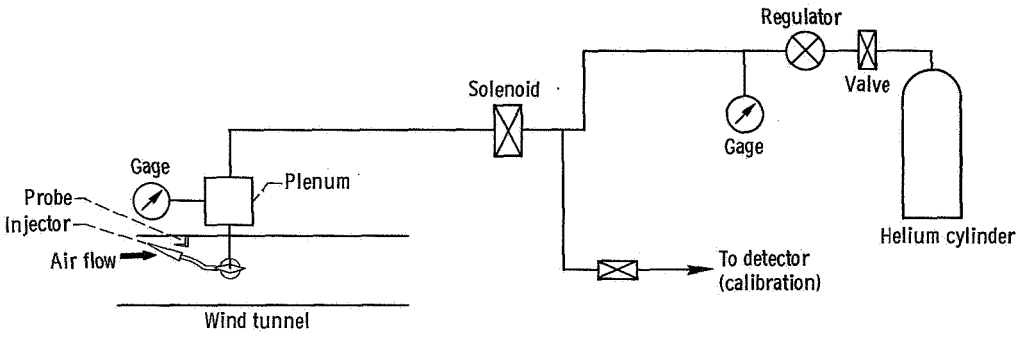

(a) Schematic of helium injection system.

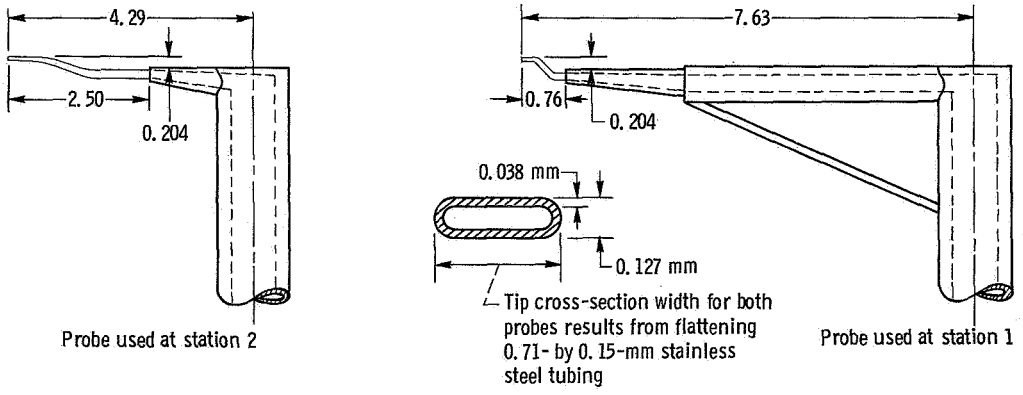

(b) Gas sampling probes. (Dimensions are in centimeters unless otherwise stated.)

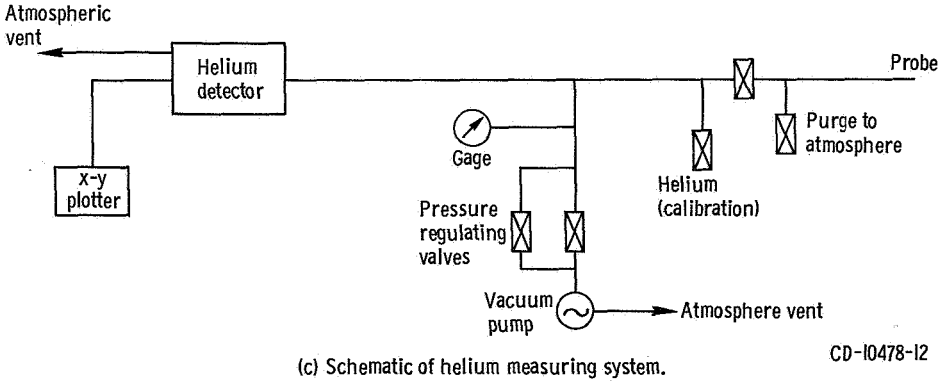

(c) Schematic of helium measuring system.

Figure 3. - Gas sampling apparatus.

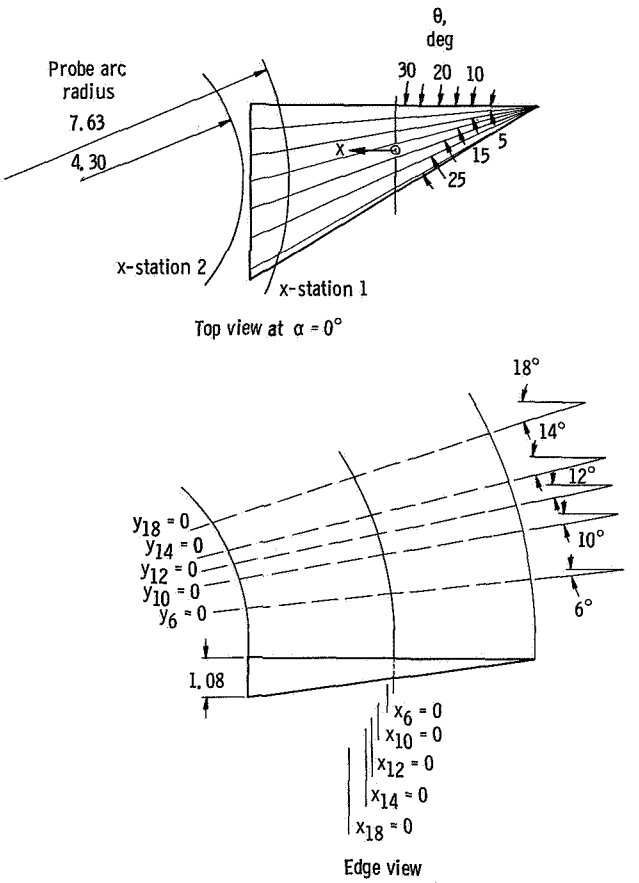

Angular position, θ, deg	Angle of attack, α, deg									
	6		10		12		14		18	
	Station									
	1	2	1	2	1	2	1	2	1	2
	Normalized downstream distance, x/d									
5	15.0	---	13.6	----	13.0	----	11.9	18.6	10.1	16.7
10	14.6	---	13.1	19.2	12.4	18.7	11.4	17.7	9.6	15.8
15	14.4	---	12.8	19.0	12.2	18.3	11.2	17.3	9.2	15.4
20	14.4	---	13.0	19.2	12.1	18.7	11.0	17.6	9.2	15.5
25	14.7	---	13.2	----	12.3	19.6	11.3	18.6	9.4	16.5
30	15.6	---	14.0	----	13.0	----	11.9	----	9.9	----

Figure 4. - Schematic of model rotation and probe measurement stations.

the y direction, normal to the free-stream direction, by means of an actuator that was calibrated in 0.001-inch (0.00254-cm) divisions. For any x and θ position, y = 0 was at the model surface.

The position change in the model with angle of attack change is shown in the edge view schematic of figure 4. Concentration measurements were obtained at 6°, 10°, 12°, 14°, and 18° angles of attack. Since the model axis of rotation was located behind the trailing edge, the distance from the injection orifice to the probe changed with each angle of attack. A table of x/d values for various probe positions is included in figure 4. Also, the angular position θ, at which the probe arcs intersect a line drawn straight downstream from the orifice, changed with angle of attack.

RESULTS AND DISCUSSION

Vortex Location

The vortex flow pattern on the model surface is shown for $\alpha = 15^{o}$ and 18^{o} in the oil-streak photographs in figure 5(a). For $\alpha = 15^{o}$ with the injection orifice plugged, the primary vortex attachment line was clearly visible to the left of the injection orifice. The boundary-layer separation line was also visible closer to the leading edge, and the typical cross-flow pattern between the attachment and separation lines was observed. The dark smear region in the lower right hand corner was caused by surface flow reversal when the tunnel was shut down. For $\alpha = 18^{o}$ with 15-psia (103.4-kN/m^2) helium injection, the same flow characteristics were observed upstream of the injection orifice. To the left and downstream of the orifice, however, two dark cross model flow patterns due to injection were present. This behavior was also noted at $\alpha = 12^{o}$ with injection. In the downstream right hand region a very distinct curved line indicated leading edge flow

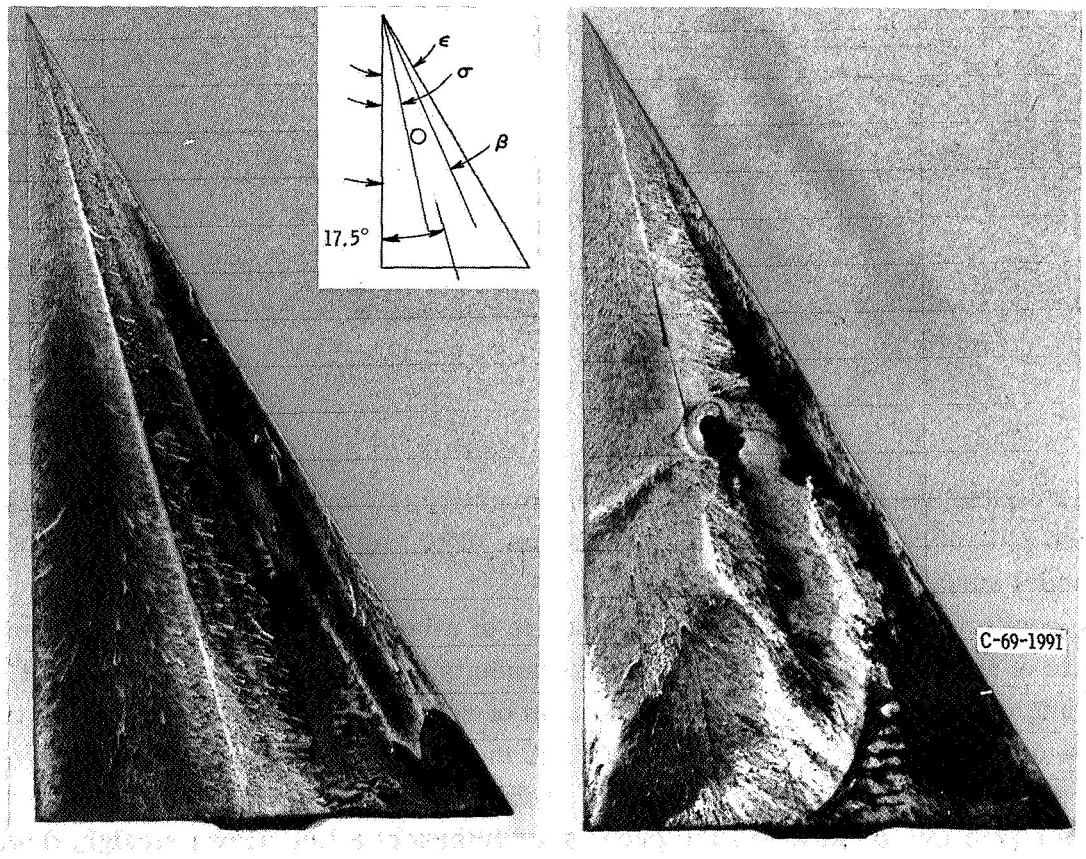

Angle of attack, 15°; no injection

Angle of attack, 18°; 15-psia (103.4-kN/m^2) injection

(a) Oil streak photographs.

Figure 5. - Determination of vortex position on model surface.

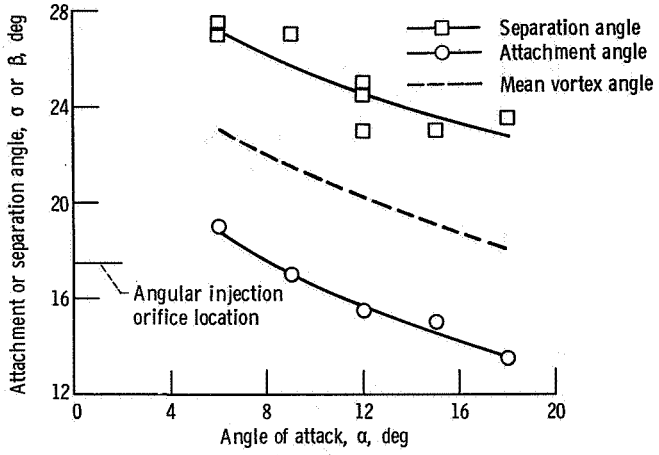

(b) Measured angles.

Figure 5. - Concluded.

separation, which altered the flow behavior over the model at x-station 2. This separation was noted only at $\alpha = 18^{\circ}$. The total angle of attack to the flow of the bottom surface of the model was 26° (18° plus 8° wedge angle). The two-dimensional wedge shock separation angle is 23°. Schlieren observation, however, showed that the compression shock was still attached to the apex of the model. Thus the swept leading edge apparently delayed shock detachment and did not cause leading-edge separation until approximately two-thirds of the distance along the leading edge. Concentration measurements at x-station 1 were upstream of this flow separation and appeared to be unaffected.

Measurements of the attachment and boundary-layer separation angles were made from the oil-streak photographs and are shown in figure 5(b) as a function of angle of attack. Vortex size remained approximately constant in width but moved inboard with increasing angle of attack. The mean vortex angle was taken to be midway between the attachment and separation angles.

Concentration Measurements

An example of typical helium concentration data obtained from a traverse in the y direction is shown in figure 6 for one set of conditions: $\alpha = 6^{\circ}$, $\theta = 12.5^{\circ}$, and $P_o = 15$ psia (103.4 kN/m^2). Distance above the model surface normalized by the injection orifice diameter y/d is shown plotted against percent helium concentration. The intersection of a faired curve (fig. 6) with the ordinate was taken as zero percent helium. The y/d value of this intercept is defined as the penetration. The penetration was determined to be accurate to within at least a y/d value of ± 0.25 or half the distance between the zero and first nonzero concentration measurements.

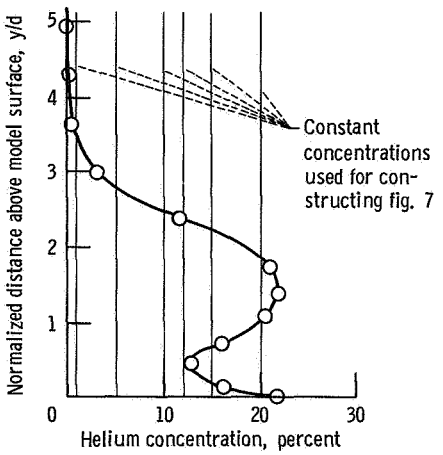

Figure 6. - Helium concentration profile at x-station 1. Angle of attack, 6°; angular position, 12.5°; injection total pressure, 15 psia (103.4 kN/m^2).

Crossplotting the helium profiles as y/d against θ resulted in constant concentration contours as shown typically in figure 7. The data points on the contours were obtained in crossplotting and do not necessarily correspond to measurement locations. These points are included to indicate how much interpretation was used to construct the contour plots. These contours represent an overall picture of the helium distribution above the model on a cylindrical surface described by the probe arc and vertical traverses.

Angle of attack effect. - Figure 7 shows the helium concentration contours at x-station 1 for an injection pressure of 15 psia (103.4 kN/m^2) and angles of attack of 6°, 10°, 12°, 14°, and 18°. At all angles of attack, the highest concentration and maximum penetration of helium were observed in a region approximately in line with the injection orifice at an angular position of from 9° to 11°. (In line will be used to mean directly downstream in the free-stream flow direction.) The jet contours were skewed relative to those measured in reference 5 for a jet injected from a flat plate at $\alpha = 0^\circ$. At $\alpha = 6^\circ$ (fig. 7(a)) very little helium was picked up and spread into the vortex region, but at $\alpha = 10^\circ$ and greater (fig. 7(b) to (e)) large concentrations of helium were found carried into the vortex. High concentrations were also found over an angular range from approximately 20° to 28° at angles of attack greater than 6°. This region corresponded to the secondary vortex and separation region discussed in reference 6 and to the location of the boundary-layer separation line measured from the oil-streak photographs (fig. 5). The maximum concentration in this region increased with increasing angle of attack. From figure 5(b) it can be seen that only for $\alpha = 6^\circ$ was the jet injected outside of the vortex flow. Thus for any appreciable increase in lateral distribution at small x/d distances, the injection orifice should be located so that the gas is initially injected into some portion of the vortex.

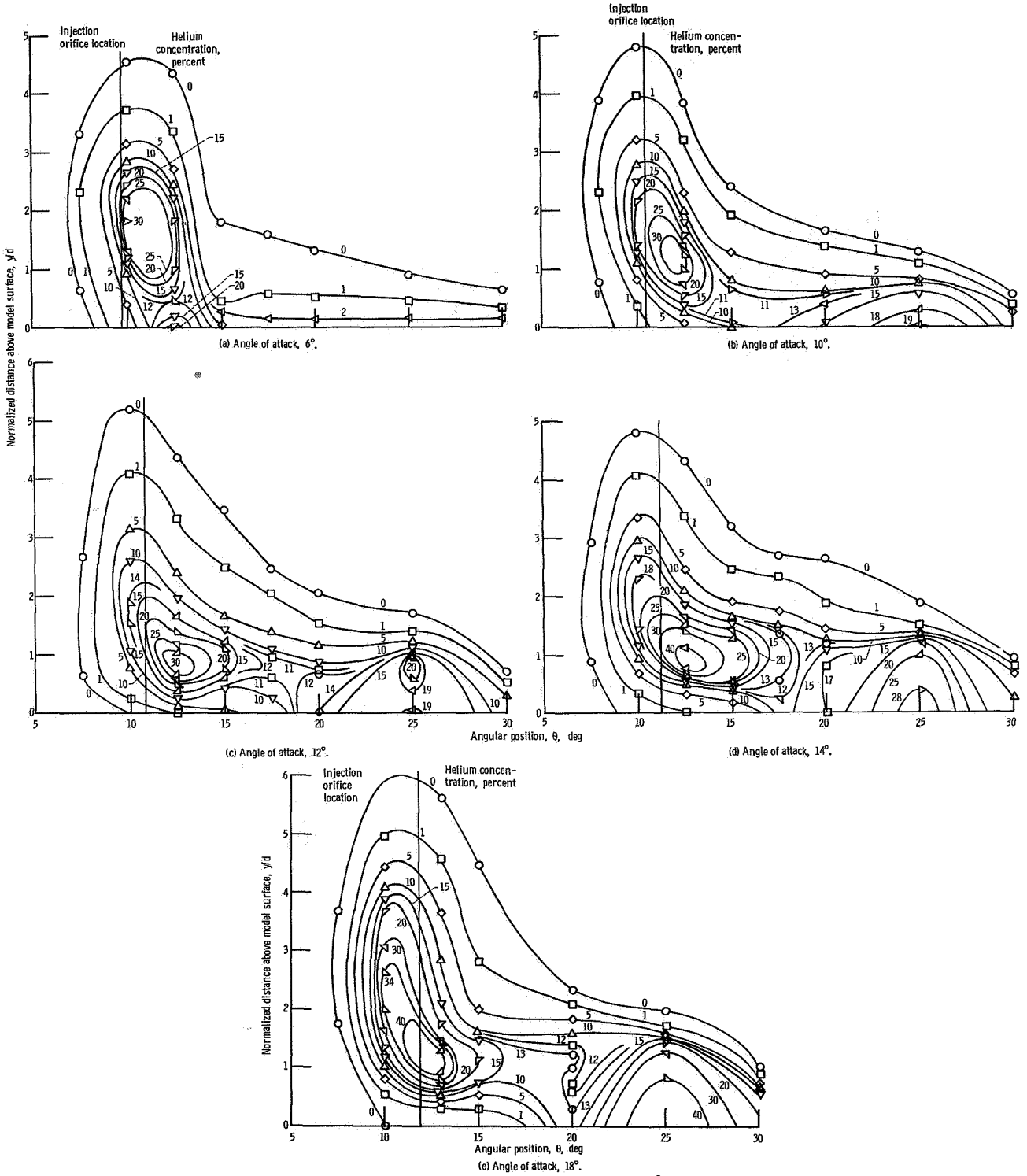

(a) Angle of attack, 6°.

(b) Angle of attack, 10°.

(c) Angle of attack, 12°.

(d) Angle of attack, 14°.

(e) Angle of attack, 18°.

Figure 7. - Constant concentration contours. x-station 1; injection pressure, 15 psia (103.4 kN/m^2. (Data points result from crossplotting.

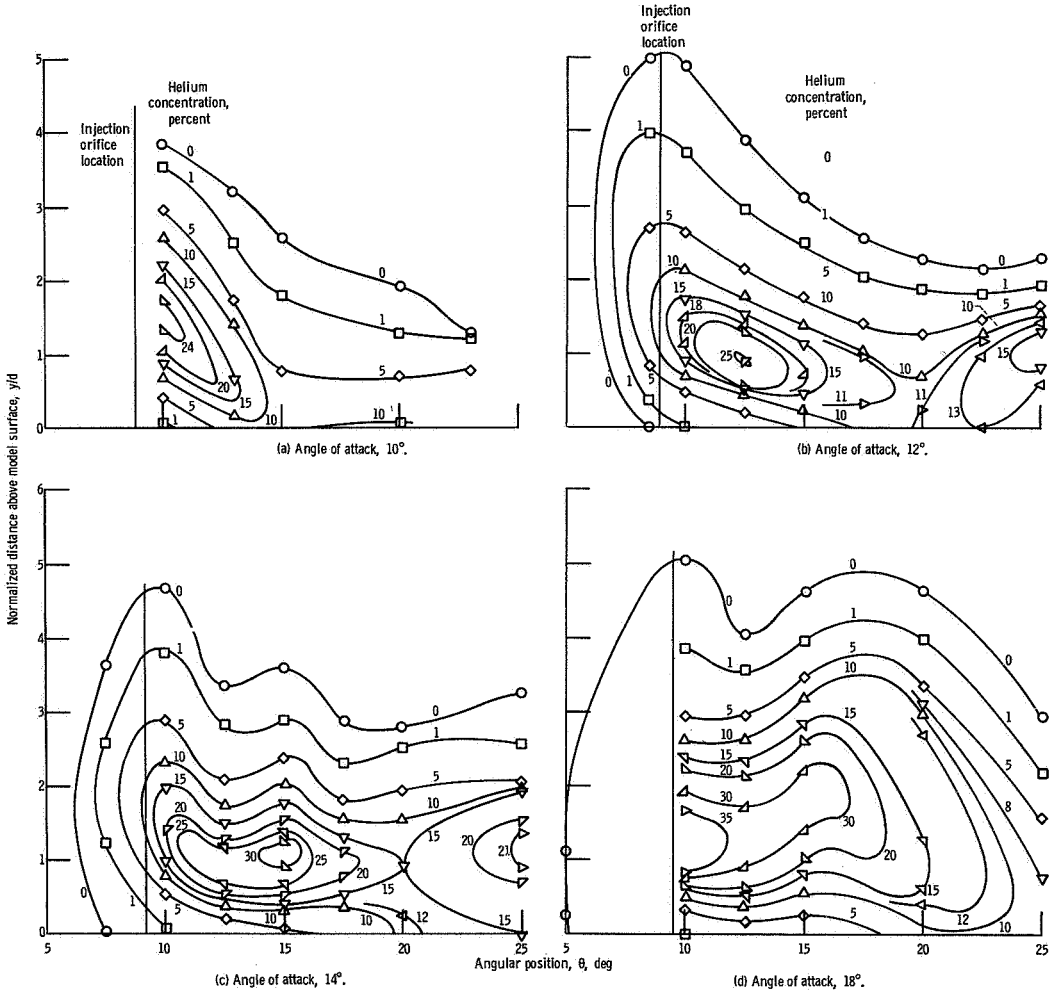

Figure 8. - Constant concentration contours. x-station 2; injection pressure, 15 psia (103.4 kN/m^2). (Data points result from crossplotting.)

The qualitative jet behavior at x-station 2 for P_o = 15 psia (103.4 kN/m^2) (fig. 8) was the same as that upstream at x-station 1. The jet still was skewed to the vortex region and more lateral distribution occurred as angle of attack was increased. The marked change in behavior at $\alpha = 18^o$ was due to the flow separation which occurred (see fig. 5(a)). The penetration in the vortex region was nearly as great as that in line with the injection orifice.

In order to make comparisons of the helium boundaries in a more understandable fashion, the outer boundary (zero percent) contours have been extracted from figures 7 and 8 and replotted in figure 9. Figure 9(a) compares the zero percent helium boundaries at x-station 1 with changes in angle of attack. Although there is some crossing over of

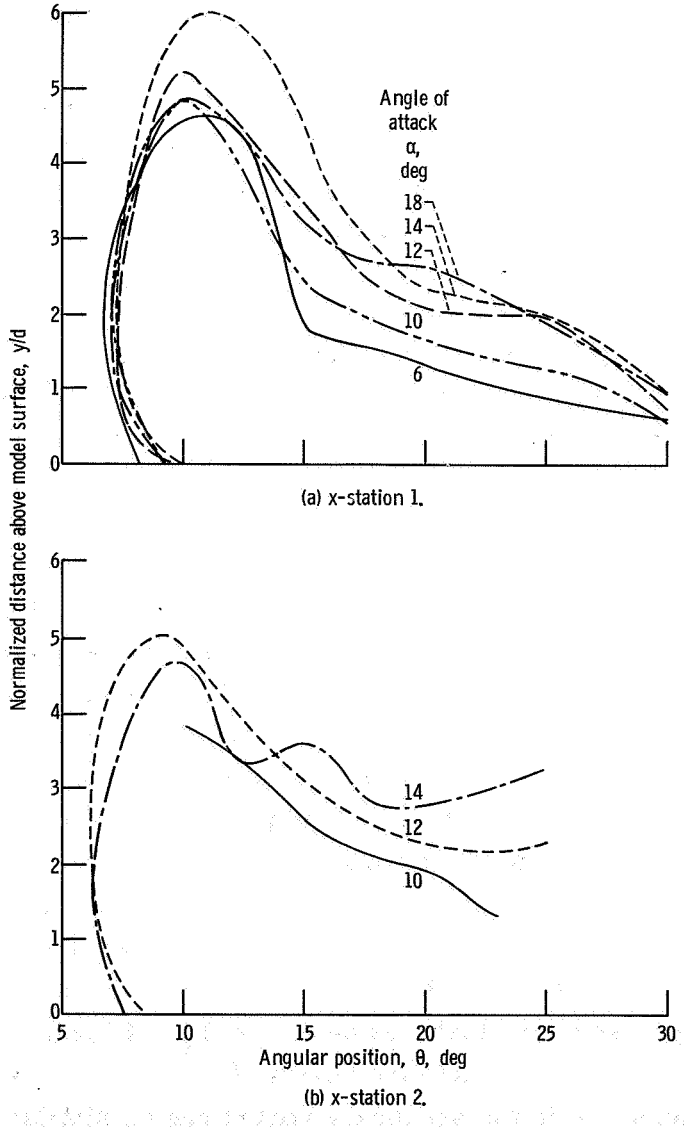

Figure 9. - Effect of angle of attack on zero percent helium boundaries. Injection pressure, 15 psia (103.4 kN/m^2).

the boundaries, there is a distinct trend of increasing penetration with increasing angle of attack over most of the model surface. An increased penetration in line with the injection orifice might be expected from purely a momentum argument since the ratio of jet momentum to the local free-stream momentum over the model surface increased with increased angle of attack. The flow pattern over the delta, however, was complicated by vortex formation and surface injection, thus making it difficult to predict the overall penetration gain.

At x-station 2, figure 9(b) the outer boundaries are compared at $\alpha = 10^{\circ}$, 12°, and 14°. The $\alpha = 18^{\circ}$ data have not been included because of the flow separation. Qualitatively, the penetration behavior was similar to x-station 1; however, the crossing of the curves complicated the picture in line with the injection orifice. Most of this crossover can be attributed to the accuracy with which the zero concentration boundary can be determined. If the 1- or 5-percent concentration boundaries are considered from figures 7 and 8, the penetration behaves more regularly with increasing angle of attack.

A representation of the zero-percent helium boundary is shown to scale in an isometric view (fig. 10). The model is shown at $\alpha = 14^{\circ}$. The lateral spreading was 2.5 to 3 times greater than the penetration height for the zero-percent boundary. The 20-percent helium boundary is also shown.

Effect of normalized downstream distance. - An evaluation of the change in penetration with x/d is made in figure 11. Here θ positions where concentration measurements were made have been chosen for comparison to eliminate any uncertainty due to drawing of the contours. The straight lines drawn through the data points were assumed to be representative of the zero boundary trajectory. Generally, there was little change in penetration with downstream distance over the short distance measured. The trend seems to be a decrease in penetration nearly in line with the injection orifice and an increase in penetration with increasing x/d at the outboard locations. Thus there was indication that, as the jet progressed downstream, the vortex pulled the jet outboard more into the vortex region. This effect was noticed at 10°, 12°, and 14° angles of attack even though the injection hole location changed relative to the vortex with a change in α (fig. 5). Thus a small change in injection orifice location is not expected to appreciably affect these x/d results. Again, most of the crossover in the penetration curves with x/d can be attributed to the accuracy of the zero concentration boundary.

Injection pressure effect. - The helium concentration contours obtained at x-station 1 for a higher injection pressure of 60 psia (413.7 kN/m^2) are shown in figure 12. Angles of attack of 6° and 18° are presented. The penetration and the maximum concentration measured have both increased over that measured for $P_o = 15$ psia (103.4 kN/m^2). At $\alpha = 6^{\circ}$ very little helium was spread into the vortex, but at $\alpha = 18^{\circ}$ significant helium concentrations were measured in the secondary vortex region similar to the lower injection pressure results.

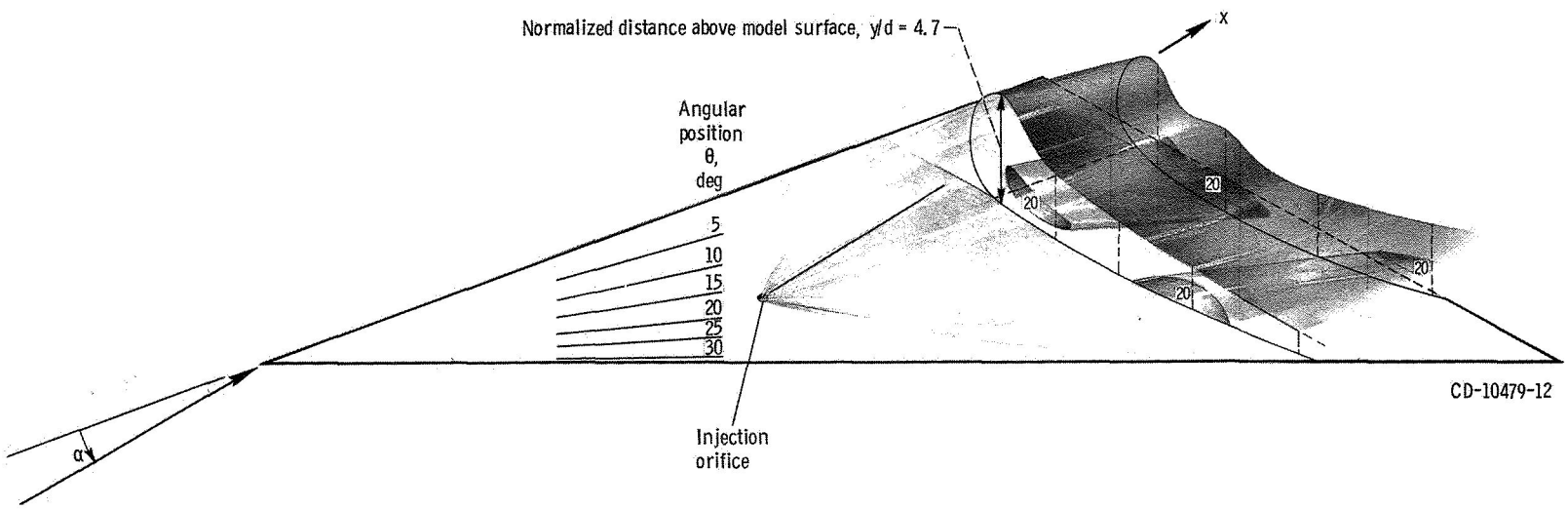

Figure 10. - Isometric of zero percent helium boundary for model at 14° angle of attack. Injection pressure, 15 psia (103.4 kN/m^2).

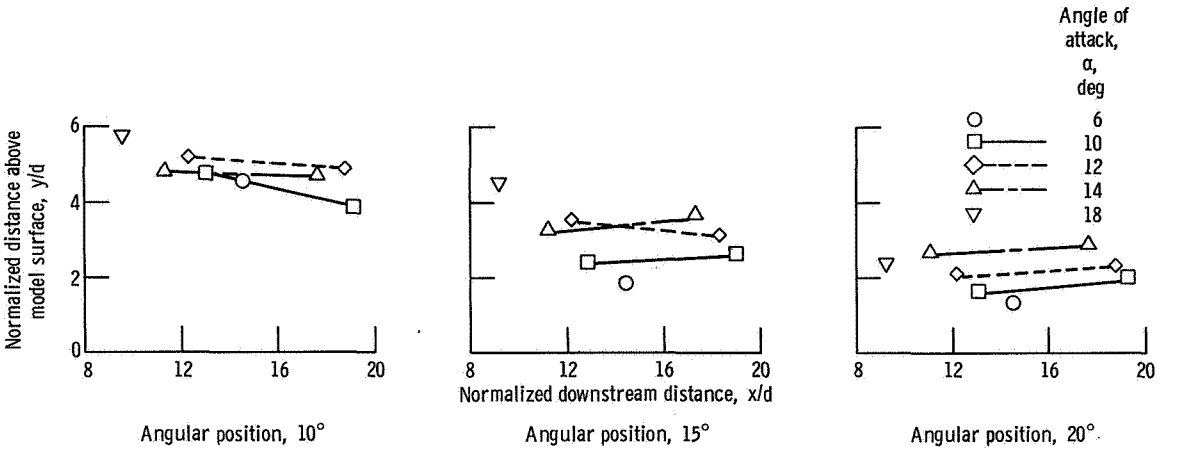

Figure 11. - Change in penetration of zero percent helium boundary with downstream distance at various angular positions. Injection pressure, 15 psia (103.4 kN/m^2).

The zero-percent helium boundaries reconstructed from figure 12 for 60-psia (413.7-kN/m^2) injection pressure are compared with the 15-psia (103.4-kN/m^2) boundaries in figure 13. Comparison is made for $\alpha = 6^o$ (fig. 13 (a)) and $\alpha = 18^o$ (fig. 13 (b)). At both angles of attack the penetration in line with the injection orifice approximately doubled, but in the vortex region no significant increase in penetration was noted. The spreading to the nonvortex side of the injector increased slightly (about 4^o) with the higher pressure.

The injection pressure effect on penetration is shown for θ positions of 10^o, 15^o, and 20^o in figure 14. Again, it can be seen that at larger θ values the pressure effect on penetration decreased. At $\theta = 10^o$, approximately in line with the injection orifice, injection pressure had a greater effect on penetration than did angle of attack. Conversely, at $\theta = 20^o$, approximately the vortex position, an increase in α increased penetration, while pressure had negligible effect. Increasing the injection pressure did not increase the concentration of helium in the vortex region, but rather the influence was seen approximately in line with the injection orifice.

Comparison With Mean Vortex Position

The location of the mean vortex above delta surfaces was predicted from a potential solution in reference 6. A comparison of the measured penetrations with the mean vortex positions were made in figure 15 for the various angles of attack. The measured penetration values were determined from figures 7, 8, and 12 at the vortex angles obtained from the oil-streak photographic data of figure 5. From the limited x/d data it appeared as though a correspondence existed between measured penetration and predicted vortex

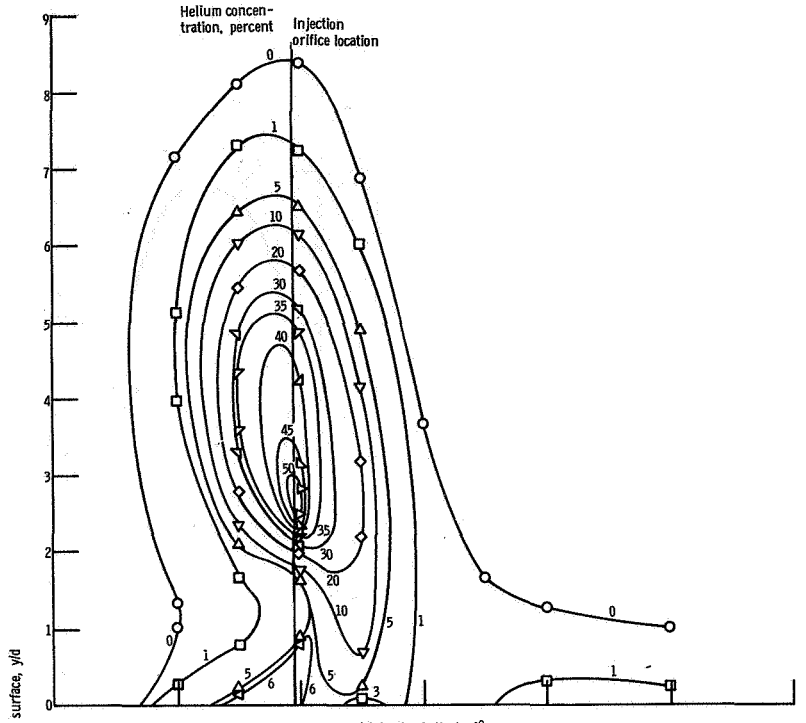

(a) Angle of attack, 6°.

(b) Angle of attack, 18°.

Figure 12. - Constant concentration contours, x-station 1; injection pressure, 60 psia (413.7 kN/m^2. (Data points result from crossplotting).

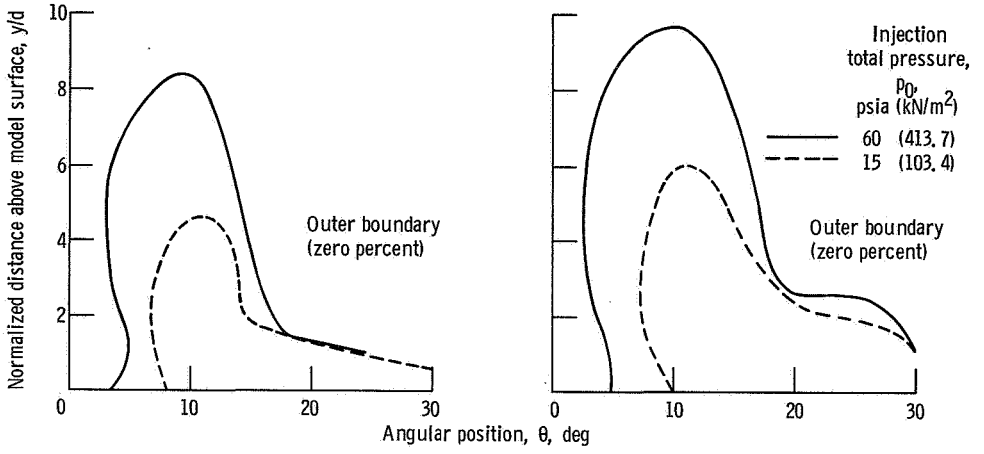

(a) Angle of attack, 6°.

(b) Angle of attack, 18°.

Figure 13. - Effect of injection pressure on zero percent helium boundaries. x-station 1.

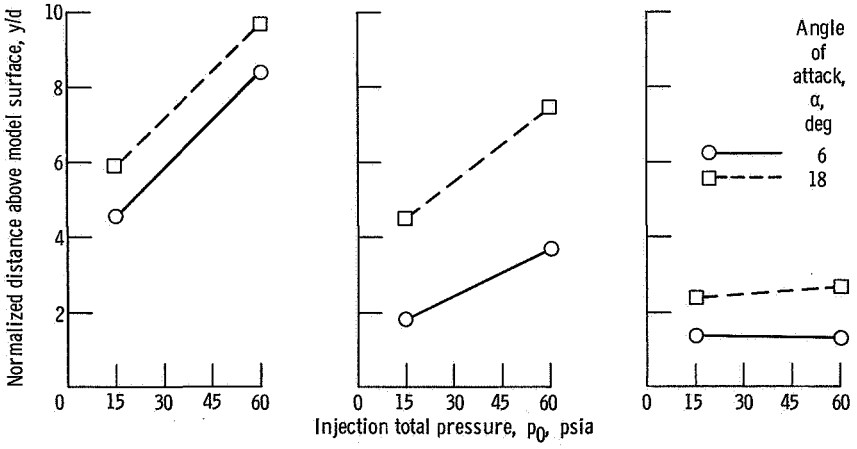

(a) Angular position, 10°.

(b) Angular position, 15°.

(c) Angular position, 20°.

Figure 14. - Effect of injection pressure on penetration at various angular positions. x-station 1.

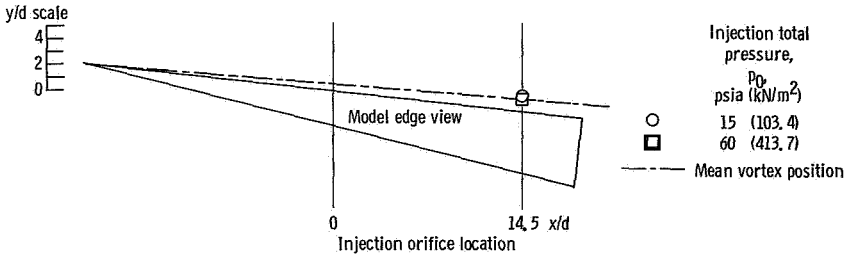

(a) Angle of attack, 6°; angular position, 23°.

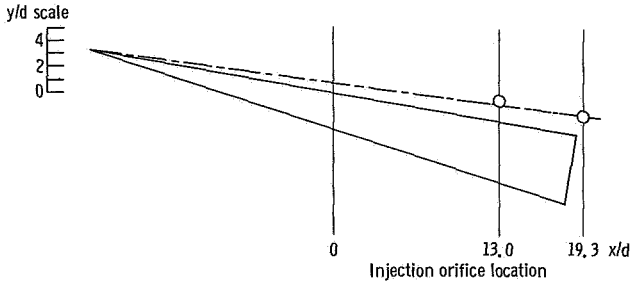

(b) Angle of attack, 10°; angular position, 21°.

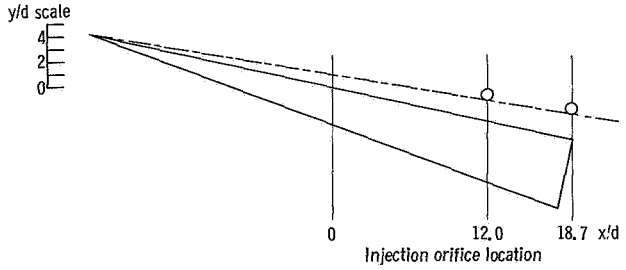

(c) Angle of attack, 12°; angular position, 20°.

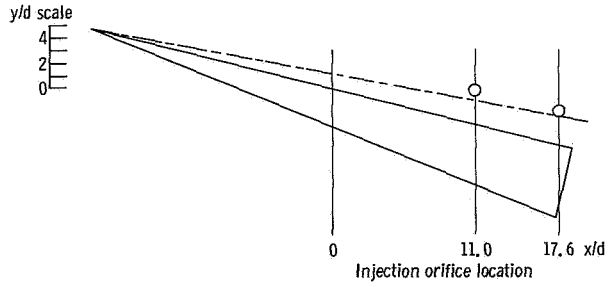

(d) Angle of attack, 14°; angular position, 19.5°.

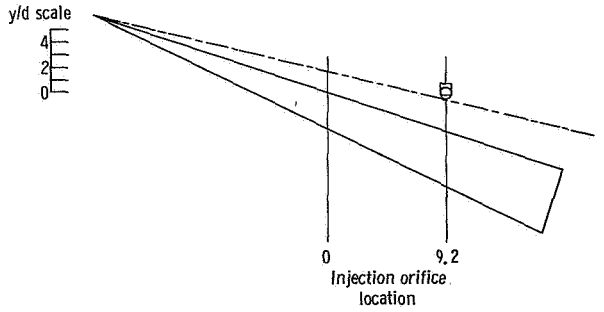

(e) Angle of attack, 18°; angular position, 18°.

Figure 15. - Comparison of measured penetration with mean vortex position from potential solution.

height for all angles of attack and both injection pressures. Comparison of the measured jet boundary with the vortex position was also made in reference 4 for $\alpha = 12^{\circ}$ and $P_0 = 15$ psia (103.4 kN/m^2), and agreement was also found to exist over the model surface and slightly downstream ($x/d \leq 20$) of the trailing edge.

Relevance to Supersonic Combustion Ramjets

For an engine injector configuration, penetration and spreading of the injected jet would only be part of the necessary considerations. Injection techniques would need to be evaluated in terms of completeness of combustion and overall performance. To warrant incorporation of injectors of the type used in this study the total pressure loss and drag due to injection and injector devices would have to be offset by increased overall efficiency. Injector drag would be approximately proportional to α^2. This particular study has characterized the injected flow in the near field over a half-delta configuration, which may or may not constitute a reasonable injector design. It may be possible to use other configurations such as swept struts at angle of attack to generate vortex flow (ref. 4) where a major portion of the flow over the strut may be at the vortex angle. Ultimately, the jet distribution in the far field ($x/d > 100$) would be desired.

SUMMARY OF RESULTS

Concentration measurements were made downstream of the injection of a secondary gas into a supersonic airstream from a half-delta model. Model angle of attack and injection pressure were varied. Penetration of the zero percent helium boundary increased with increasing angle of attack and injection pressure. Approximately in line with the injection orifice, increasing injection pressure had a greater effect on penetration than did an increase in angle of attack. Conversely, approximately at the vortex position, an increase in angle of attack increased penetration while pressure had a negligible effect. Greatest penetration was obtained for the higher injection pressure at the largest angle of attack.

At angles of attack of 10° and greater, large concentrations were observed in the vortex region. At a 6° angle of attack, where the jet was injected outside the vortex flow, very little helium was picked up and spread into the vortex region. This behavior was observed at both injection pressures.

Downstream distance over the model surface had little effect on penetration. However, the trends indicated that, as the jet progressed downstream, the vortex pulled the jet outboard more into the vortex region.

Measured zero concentration boundaries were in agreement with the locations of the mean vortex predicted from a potential solution.

Lewis Research Center,
National Aeronautics and Space Administration,
Cleveland, Ohio, June 24, 1969,
722-03-00-06-22.

REFERENCES

1. Orth, Richard C.; and Funk, John A.: An Experimental and Comparative Study of Jet Penetration in Supersonic Flow. J. Spacecraft Rockets, vol. 4, no. 9, Sept. 1967, pp. 1236-1242.

2. Schetz, Joseph A.; and Gilreath, Harold E.: Tangential Slot Injection in Supersonic Flow. AIAA J., vol. 5, no. 12, Dec. 1967, pp. 2149-2154.

3. Vranos, A.; and Nolan, J. J.: Supersonic Mixing of a Light Gas and Air. Presented at the AIAA Propulsion Joint Specialist Conference, Colorado Springs, Colo., June 14-18, 1965.

4. Povinelli, Louis A.; Povinelli, Frederick P.; and Hersch, Martin: A Study of Helium Penetration and Spreading in a Mach 2 Airstream Using a Delta Wing Injector. NASA TN D-5322, 1969.

5. Torrence, Marvin G.: Concentration Measurements of an Injected Gas in a Supersonic Stream. NASA TN D-3860, 1967.

6. Pershing, Bernard: Separated Flow Past Slender Delta Wings with Secondary Vortex Simulation. Rep. TDR-269(4560-10)-4, Aerospace Corp. (SSD-TDR-64-151, DDC No. AD-607442), Aug. 24, 1964.

1. Report No. NASA TM X-1889	2. Government Accession No.	3. Recipient's Catalog No.
4. Title and Subtitle EFFECT OF ANGLE OF ATTACK AND INJECTION PRESSURE ON JET PENETRATION AND SPREADING FROM A DELTA WING IN SUPERSONIC FLOW		5. Report Date September 1969 6. Performing Organization Code
7. Author(s) Frederick P. Povinelli, Louis A. Povinelli, and Martin Hersch		8. Performing Organization Report No. E-5080
9. Performing Organization Name and Address Lewis Research Center National Aeronautics and Space Administration Cleveland, Ohio 44135		10. Work Unit No. 722-03-00-06-22. 11. Contract or Grant No.
12. Sponsoring Agency Name and Address National Aeronautics and Space Administration Washington, D.C. 20546		13. Type of Report and Period Covered Technical Memorandum 14. Sponsoring Agency Code
15. Supplementary Notes		

16. Abstract

Helium injection into the vortex flow generated over the lee side of a half-delta model was studied in a Mach 2 airstream. Concentration contours were obtained at two positions downstream of the injection orifice. Angle of attack and injection pressure were varied. Oil-streak photographic data were used to determine the location of the vortex on the delta surface. Penetration and spreading of the injectant were enhanced with increasing angle of attack. Increasing injection pressure increased the penetration but had little effect on spreading. Maximum penetration occurred at the highest angle of attack and injection pressure tested.

17. Key Words (Suggested by Author(s))	18. Distribution Statement
Jet Penetration Jet Spreading Supersonic Flow Delta Wing Concentration Profiles Injection Pressure Angle of Attack Vortex Flow Mixing	Unclassified - unlimited

19. Security Classif. (of this report)	20. Security Classif. (of this page)	21. No. of Pages	22. Price*
Unclassified	Unclassified	22	$3.00

*For sale by the Clearinghouse for Federal Scientific and Technical Information Springfield, Virginia 22151

"The aeronautical and space activities of the United States shall be conducted so as to contribute . . . to the expansion of human knowledge of phenomena in the atmosphere and space. The Administration shall provide for the widest practicable and appropriate dissemination of information concerning its activities and the results thereof."

—NATIONAL AERONAUTICS AND SPACE ACT OF 1958

NASA SCIENTIFIC AND TECHNICAL PUBLICATIONS

TECHNICAL REPORTS: Scientific and technical information considered important, complete, and a lasting contribution to existing knowledge.

TECHNICAL NOTES: Information less broad in scope but nevertheless of importance as a contribution to existing knowledge.

TECHNICAL MEMORANDUMS: Information receiving limited distribution because of preliminary data, security classification, or other reasons.

CONTRACTOR REPORTS: Scientific and technical information generated under a NASA contract or grant and considered an important contribution to existing knowledge.

TECHNICAL TRANSLATIONS: Information published in a foreign language considered to merit NASA distribution in English.

SPECIAL PUBLICATIONS: Information derived from or of value to NASA activities. Publications include conference proceedings, monographs, data compilations, handbooks, sourcebooks, and special bibliographies.

TECHNOLOGY UTILIZATION PUBLICATIONS: Information on technology used by NASA that may be of particular interest in commercial and other non-aerospace applications. Publications include Tech Briefs, Technology Utilization Reports and Notes, and Technology Surveys.

Details on the availability of these publications may be obtained from:

SCIENTIFIC AND TECHNICAL INFORMATION DIVISION

NATIONAL AERONAUTICS AND SPACE ADMINISTRATION

Washington, D.C. 20546